SiO maser emission from red supergiants across the Galaxy: I. Targets in massive star clusters

L. Verheyen[*], M. Messineo, and K. M. Menten

Max-Planck-Institut für Radioastronomie, Auf dem Hügel 69, D-53121 Bonn, Germany
e-mail: `verheyen, messineo, kmenten@mpifr-bonn.mpg.de`

ABSTRACT

Aims. Red supergiants (RSGs) are among the most luminous of all stars, easily detectable in external galaxies, and may ideally serve as kinematic tracers of Galactic structure. Some RSGs are surrounded by circumstellar envelopes detectable by their dust and molecular and, in particular, maser emission. This study consists of a search for maser emission from silicon monoxide (SiO) toward a significant number of RSGs that are members of massive stellar clusters, many of which have only recently been discovered. Further, we aim to relate the occurrence of maser action to properties of the host stars.
Methods. Using the IRAM 30 meter telescope, we searched for maser emission in the $J = 2 - 1$ rotational transition within the first vibrationally excited state of SiO toward a sample of 88 RSGs.
Results. With an average rms noise level of 0.25 Jy, we detected maser emission in 15% of the sample, toward most of the sources for the first time in this transition. The peak of the emission provides accurate radial velocities for the RSGs. The dependence of the detection rate on infrared colors supports a radiative pumping mechanism for the SiO masers.

Key words. Stars: AGB and post-AGB – circumstellar matter – masers

1. Introduction

Near the end of their lifetimes, stars of moderately high mass ($10\ M_\odot < M_* < 30\ M_\odot$) go through the red supergiant evolutionary phase. Red supergiants (RSGs) are burning helium in their core, have luminosities more than 10^5 times that of the Sun and, since their effective temperature is low ($\sim$ 3000–4000 K), are intrinsically luminous in the near-infrared range (NIR) (Levesque 2010). Studying RSGs and, in particular, their mass-loss history, is important for several reasons. Given their luminosities, RSGs may be recognized as individual objects in external galaxies and serve as tracers of young populations and as distance indicators. They contribute to the enrichment of the interstellar medium by losing mass at a high rate (up to several times $10^{-4}\ M_\odot\ \mathrm{yr}^{-1}$), and by eventually exploding as core-collapse supernovae. RSG stars are often surrounded by circumstellar envelopes (CSEs). Maser emission may arise from these envelopes, revealing stellar line-of-sight velocities to within a few km s^{-1} (Jewell et al. 1991). Frequently detected maser lines are from OH at 1.612 GHz, H$_2$O at 22.2 GHz, and SiO at 43 GHz and 86 GHz. At higher frequencies, also a number of (sub)millimeter transitions have been detected (see, e.g. Humphreys 2007; Menten et al. 2008).

Some fundamental issues limit the use of RSGs as well-calibrated tracers of young stellar populations. We know only about 500 RSGs (e.g. Messineo et al. 2012; Figer et al. 2006; Davies et al. 2007), and their properties (stellar and circumstellar) are still poorly understood. Interstellar extinction and poor knowledge on stellar distances render the identification of RSGs difficult. Important open questions are those of the relations (i) between the maximum luminosity of a given star and its main-sequence mass and (ii) between mass-loss rate, $\dot{M}$, and stellar luminosity, L_* and initial metallicity, Z. Possible stellar rotation complicates these relations (Meynet & Maeder 2000). Periodic stellar light variations and circumstellar extinction make it difficult to distinguish between massive RSGs and intermediate age mass-losing late-type stars (Comerón et al. 2004; Messineo et al. 2005, 2012).

All these uncertainties limit our understanding of these stars' CSEs. In particular, it is unclear why some stars exhibit maser emission in a certain species and others don't. Maser occurrence is certainly not only a function of envelope temperature and mass-loss rate alone; other parameters, like elemental abundances and stellar luminosity may play an important role (Habing 1996).

Large-scale searches for maser emission toward evolved late-type stars (mostly Mira-type long period variables and OH/IR stars) have been carried out, successfully yielding radial velocity measurements, and new views on the structure of the Milky Way, in particular on its bar and bulge (Sevenster 1999; Deguchi et al. 2002; Habing et al. 2006). The power of velocity determinations via observations of SiO maser lines was demonstrated by Messineo et al. (2002, 2004, 2005) and Habing et al. (2006),

---

who used the IRAM 30m telescope to find 86 GHz SiO maser emission toward 271 color-selected AGB stars in the Inner Galaxy with a detection rate higher than 60%. With ages of up to a few tens of Myr, the much younger RSGs, on the other hand, are found in the general vicinity of their birth places.

Recently, trigonometric parallaxes of maser sources in star-forming regions and toward a few RSGs located in the spiral arms of the Milky Way have been measured with the NRAO Very Long Baseline Array (VLBA) and VLBI Exploration of Radio Astrometry (VERA) with a precision of 10%. These accurate distances are leading to a revised view of Galactic structure (Reid et al. 2009; Choi et al. 2008; Asaki et al. 2010). RSGs are found in the spiral arms and their associated masers are thus excellent potential targets for such studies. In fact, one purpose of the present work is to increase the number of RSG/SiO maser sources suitable for Very Long Baseline Interferometry (VLBI).

In order to use RSGs as kinematic probes, it is necessary to significantly increase the number of such objects with known associated maser emission. Strong masers (with hundreds to > thousand Jy intensities) were first detected in nearby "classical" OH/IR RSGs (VY CMa, VX Sgr, NML Cyg, and also S Per) in the early 1970s (Buhl et al. 1974; Kaifu et al. 1975). Searches for RSG masers in the far reaches of the Galaxy require sensitive searches with few- to even sub-Jy sensitivity.

In this paper, we present a search for 86 GHz SiO maser emission toward 88 known RSG stars associated with open clusters.

In Sect. 2, we report recent discoveries of massive clusters that have RSGs amongst their members (the so named Red Supergiant Clusters, RSGCs), and in Sect. 3 give a brief summary of SiO maser emission and the motivation for its study. The observations are described in Sect. 4. General results are presented in Sect. 5, discussed, cluster by cluster, in Sect. 6 and analyzed in Sect. 7. Some conclusions are presented in Sect. 8.

2. Red supergiants in stellar clusters

Ideally, one wishes to observe RSG stars in clusters, because membership in a stellar cluster guarantees similar distance, age and metallicity for all its constituents, including the RSGs. The RSGs' distinct properties, compared to other cluster members, will thus only depend on their large initial masses. Due to the steepness of the initial mass function stellar clusters rich in RSGs must naturally be very massive, and have an age from about 5 to 30 Myr (Meynet & Maeder 2000).

Only 15 massive clusters (mass $> 10^4\ M_\odot$) are currently known in the Milky Way (the most recently found ones reported by Messineo et al. 2009; Negueruela et al. 2010, 2011; Messineo et al. 2012). They are all located at the near-side of the Galaxy, suggesting that their census is highly incomplete (Messineo et al. 2009). A few clusters, e.g. the Westerlund I, Arches, and Quintuplet clusters (Westerlund 1961; Cotera et al. 1996; Figer et al. 1999, 2002, 2004; Clark et al. 2005) were known to be massive since the 1990s or even earlier and have been studied at various wavelengths. However, the Arches and the Quintuplet may not be representative of massive clusters elsewhere in the Milky Way because of the peculiar physical conditions in the Galactic center region. Thanks to the new generation of near- and mid-infrared surveys (e.g. DENIS, 2MASS, GLIMPSE, Epchtein et al. 1999; Cutri et al. 2003; Benjamin et al. 2003), recently several more massive Galactic stellar clusters containing RSGs have been discovered around $l \sim 25°$, at the base of the Scutum-Crux arm. In the Red SuperGiant Cluster 1 (RSGC1) a total of 14 RSGs have been spectroscopically confirmed (Figer et al. 2006; Davies et al. 2008). Only a few hundred parsecs from the RSGC1, another massive cluster was found. RSGC2, also called the Stephenson 2 cluster (Stephenson 1990), contains 26 RSGs (Davies et al. 2007). A nearby third massive cluster (RSGC3) with 16 RSGs was discovered by Clark et al. (2009) and Alexander et al. (2009). Recently, two other clusters rich of RSGs were identified in the same direction (Negueruela et al. 2010, 2011). The Alicante 8 or RSGC4 contains 13 candidate RSG members, while the RSGC5 cluster contains seven RSGs. Since the latter two clusters were not yet discovered at the time of the observations presented in this paper, they were not considered in our search. The total number of confirmed RSG stars in these five clusters amounts to 64, increasing the number of known RSGs by at least 15%. Before this, only the NGC 7419 cluster was known to contain five RSGs (Beauchamp et al. 1994; Caron et al. 2003). All five RSGCs are concentrated within a few degrees of longitude ($25° < l < 29°$), likely at similar distance (5–6 kpc). The location of this remarkable burst of star formation coincides with the near endpoint of the Galactic bar (Davies et al. 2009b), where also the W43 "mini starburst" region is found (Nguyen Luong et al. 2011). These clusters offer an extraordinarily important natural laboratory in which to study the evolution of RSGs and the properties of their envelopes. Altogether, we now have a sample of more than 119 Galactic RSGs in clusters at our disposal (Messineo et al. 2012). Here we present a search for 86 GHz SiO maser emission toward RSG stars.

The RSGCs are at distances of approximately 3.5 kpc from the Galactic center, all are at kinematically interesting locations, namely at the corotation radius of the Galactic bar (Habing et al. 2006), at the base of the Scutum-Crux arm, or near an endpoint of the Galactic bar. Studies of their properties and kinematics, e.g. via SiO maser emission, will place constraints on Galactic structure and evolution models and address, e.g., questions how the Galactic bar and the spiral arms are dynamically related, which is still unclear (Bissantz et al. 2003).

3. SiO masers in red supergiants

Analysis of existing photometric data (from the 2MASS, MSX, Spitzer/GLIMPSE databases) has shown that many RSGs show infrared excesses, caused by their CSEs, and therefore high mass-loss rates (e.g. Figer et al. 2006; Davies et al. 2007). Typical mass-loss rates range from 10^{-8} to $10^{-4}\ \dot{M}$ per year (Verhoelst et al. 2009; Harwit et al. 2001). This makes them likely to exhibit maser emission, as, e.g., the SiO maser flux is known to correlate with the mid-infrared continuum flux density see Sect. 3.1. Most commonly, RSGs show maser emission from OH (at 1.612 GHz), H_2O (22 GHz) and SiO (43 GHz and 86 GHz) (see e.g. Habing 1996). In this paper, we will focus on the 86 GHz SiO ($v = 1, J = 2 - 1$) maser line.

3.1. SiO maser pumping

The pumping mechanism for SiO masers is still under debate. Both radiative and collisional pumping models have been proposed. The basic mechanism for SiO maser pumping is described by Kwan & Scoville (1974). They find that SiO population inversions can occur when vibrational transitions become optically thick. Namely, in this case the vibrational de-excitation rates will be modified in such way that they decrease with increasing rotational level J. The logical result is an overpopulation of higher J rotational levels, thus an inversion, as long as the pumping happens by collisions or an indirect radiative route.

Models favoring either collisional or radiative pumping have been proposed by a number of authors. A mechanism for pumping through collisions with H_2 molecules was first presented by Elitzur (1980). Further modeling by, e.g., Lockett & Elitzur (1992) and Humphreys et al. (2002) also supported collisional pumping as the primary pumping mechanism for SiO masers. On the other hand, contrasting studies find radiative pumping to be dominant (e.g. Bujarrabal et al. 1987; Bujarrabal 1994a,b). From the observational point of view, a radiative pumping model explains the observed correlation between SiO maser intensity and the infrared emission (e.g. Bujarrabal et al. 1987), while the dependence on stellar pulsations could be explained by collisional pumping (e.g. Heske 1989). The above models find that radiative pumping requires that the infrared (IR) flux at $8\mu m$ (the equivalent wavelength of the first excited rotational level of SiO) is greater than the flux of the maser line.

3.2. Importance of SiO maser studies: obtaining accurate velocities

To summarize the above: Finding new SiO maser-hosting RSGs associated with stellar clusters, i.e., of stars in environments of similar age, metallicity, distance and interstellar extinction is useful for analyzing the occurrence of SiO maser emission in RSGs, as a function of their luminosities and mass-loss rates (Davies et al. 2008). Very importantly, maser lines provide accurate radial velocities; the midpoint of an SiO maser spectrum gives the stellar velocity with an accuracy of a few km s^{-1} (Jewell et al. 1991). In contrast, radial velocities from infrared CO absorption at 2.29 μm in Mira stars may vary with the stellar pulsation up to 15 km s^{-1} (Scholz & Wood 2000). We note, however, that for the RSGs for which we have both maser and CO absorption LSR velocity measurements, both values are quite similar; see Table 5.

With accurate radial velocities of cluster members a determination of dynamical cluster masses is possible. Furthermore, they allow a determination of kinematic distances. However, such distances are based on models of Galactic rotation, i.e., only meaningful outside of the corotation radius and may be wrong due to peculiar motions (see, e.g., Xu et al. 2006) . Given all this, a main motivation for this work is to find new samples of RSGs with SiO maser emission whose distances can be studied with VLBI. The distances thus obtainable, typically with uncertainties of 10% at 10 kpc, will greatly improve our knowledge of massive cluster properties and place more stringent constraints on Galactic structure.

Table 1. IRAM 30m observing dates

Epoch	Dates
1	2006 September 29– October 2
2	2008 May 21–23
3	2008 August 9–11

4. Observations

4.1. Pico Veleta observations

We observed the SiO v=1, J=2–1 maser transition at 86.24335 GHz in 88 sources with the IRAM 30-m telescope on Pico Veleta, Spain, during 3 epochs in 2006 September/October and 2008 May and August (Table 1). The A100 and B100 receivers were used, connected to the 256-channel low (1 MHz) resolution filterbank with 3.5 km s^{-1} spectral resolution, as well as the VESPA autocorrelator with 240 MHz bandwidth (1600 km s^{-1}) and a resolution of 40 kHz, corresponding to an adequate 0.14 km s^{-1}. We used a total power observing mode with integration times between 5 and 15 minutes per source, employing wobbler switching with a wobbler throw of 100″– 120″. This gives an rms noise around 20–65 mK in a corrected antenna temperature, T_A^*, scale, equivalent to 0.12–0.54 Jy, assuming a conversion factor from antenna temperature to flux density of 6 Jy/K. The system temperatures ranged from 90 to 300 K. We conducted telescope pointing checks every 1.5–3 h and, based on these, estimate that pointing errors are smaller than 3″, much smaller than the 29″ FWHM beam width. .

4.2. Data reduction

We reduced the data with the CLASS program, which is part of the GILDAS software package[1]. Special attention was paid to the possible confusion with the interstellar $H^{13}CN$ $J = 1 - 0$ line, which has 3 hyperfine transitions in the 240 MHz VESPA band (Messineo et al. 2002). We detected the $H^{13}CN$ line in all of the Galactic center sources from the Blum et al. (2003) sample.

4.3. Target stars

The targets of our 86 GHz observations are late-type stars that are located mostly in the directions of massive clusters containing confirmed or candidate RSGs. Our sample is presented, with the outcome of our observations in Tables 2 and 3. Table 2 gives the coordinates of the targets toward which an SiO maser was detected and the line parameters (peak flux density, rms noise, peak LSR velocity, velocity range of maser emission, and velocity-integrated flux). Table 3 reports the coordinates of the targets not detected as well as the rms noise (1σ) of the spectra. Several of our target RSGs have already been found to show SiO maser action in the $v = 1$ and/or 2, $J = 1 - 0$ lines at 43 GHz (e.g. Nakashima & Deguchi 2006), as well as the 86 GHz $v = 1, J = 2 - 1$ line (Haikala et al. 1994) or the 43 GHz lines *and* the 86 GHz line[2] (Deguchi et al. 2010).

---

[1] http://www.iram.fr/IRAMFR/GILDAS

[2] While, in oxygen-rich evolved stars, the SiO $v = 1$ and $2, J = 1 - 0$ lines have comparable intensity, the $v = 2, J = 2 - 1$

Table 2. SiO $v = 1; J = 2 - 1$ detections toward red supergiants.

Object	α_{J2000}	δ_{J2000}	S [Jy]	rms [Jy]	v_{LSR} [km s^{-1}]	v-range [km s^{-1}]	$\int S\,dv$ [Jy km s^{-1}]	Ref.
RSGC1								
FMR2006 1	18:37:56.29	-06:52:32.2	1.2	0.20	116	[112,129]	8.1±3.0	(1)
FMR2006 3	18:37:59.73	-06:53:49.4	0.6	0.18	112	[110,117]	2.4±1.2	(1)
FMR2006 4	18:37:50.90	-06:53:38.2	1.1	0.18	121	[115,130]	6.1±1.8	(1)
FMR2006 13	18:37:58.90	-06:52:32.1	1.6	0.26	113	[108,128]	14.7±3.0	(1)
X 18	18:38:01.62	-06:55:23.5	1.7	0.22	71	[69,75]	3.1±1.2	(1)
RSGC2								
Stephenson 2 DFK 2	18:39:19.60	-06:00:40.8	1.0	0.12	101	[94,113]	6.9±1.8	(2)
Stephenson 2 DFK 49	18:39:05.60	-06:04:26.6	6.0	0.14	101	[88,109]	59.0±1.8	(2)
Stephenson 2 DFK 1	18:39:02.40	-06:05:10.6	3.0	0.19	89	[71,101]	30.5±3.0	(2)
W Per	02:50:37.90	$+56$:59:00.0	3.0	0.14	-40	[-57,-29]	33.7±2.1	(3)
S Per	02:22:51.70	$+58$:35:12.0	91.1	0.21	-41	[-50,-28]	716.4±2.7	(3)
NGC 7419-MY Cep	22:54:31.66	$+60$:49:40.3	7.9	0.11	-52	[-71,-42]	64.4±1.8	(4)
MDI2009 GLIMPSE13 1	18:53:52.49	$+00$:39:31.3	7.0	0.15	71	[57,84]	67.9±2.1	(5)
Cl Trumpler 27 1	17:36:10.12	-33:29:40.6	50.3	0.27	-17	[-25,9]	260.5±4.2	(6)
IK Tau (Mira)	03:53:28.84	$+11$:24:22.6	496.2	0.27	33.3	[30,36]	1074.0±1.5	(7)
U Her (Mira)	16:25:47.69	$+18$:53:33.1	90.8	0.22	-16	[-22,-12]	248.0±1.5	(8)

Notes. Columns are (from left to right) designations of the targeted RSGs (names are taken from SIMBAD), right ascension, declination, peak flux density, rms noise, LSR velocity of peak flux density, LSR velocity range covered by maser emission (from a Gaussian fit), velocity-integrated flux density, and a reference number.

References. (1) RSGC1 (Figer et al. 2006); (2) RSGC2 (Davies et al. 2007); (3) Per OB1 (Pierce et al. 2000); (4) NGC 7419 (Caron et al. 2003); (5) GLIMPSE13 (Messineo et al. 2009); (6) Trumpler 27 (Massey et al. 2001); (7) IK Tau; (8) U Her.

Since SiO maser emission is often variable (e.g Alcolea et al. 1990, 1999), a second epoch of observations may reveal new sources as maser emitters even if previous searches had shown negative results.

5. General Results

We searched 88 (candidate) RSGs for 86 GHz SiO maser emission. We have detected SiO maser emission from RSGs in the RSGC1 and RSGC2, NGC 7419, GLIMPSE13, and Trumpler 27 clusters, and from two RSGs in the Perseus OB1 association, S Per and W Per, which were already known to harbor SiO masers (Kaifu et al. 1975; Jiang et al. 1996). In total, 13 out of the 88 observed RSGs were found to exhibit SiO maser emission in the $v = 1, J = 2 - 1$ transition at 86 GHz.

All spectra are presented in Figure 1 and the observed line parameter are listed in Table 2. The columns specify the RSG's name (taken from SIMBAD[3]), its position by right ascension (α_{J2000}) and declination (δ_{J2000}), the peak flux density (S, in Jy), the rms noise (rms, in Jy), the LSR velocity of the peak flux density (v_{LSR}, in km s^{-1}), the LSR velocity range covered by the maser emission (v-range, in km s^{-1}), the velocity-integrated flux density ($\int S\,dv$, in Jy km s^{-1}), and a reference number. Table 3 lists upper limits for sources toward which no maser emission was found. The columns specify the RSG's name (taken from SIMBAD), its position by right ascension (α_{J2000}) and declination (δ_{J2000}), and the rms noise (rms, in Jy).

Toward several of the 13 sources in which we detect SiO maser emission SiO, OH and/or H_2 masers had been found

previously. For these, Table 4 gives an overview of all the maser detections.

6. Results on individual clusters

In the following we discuss our targets and our observations cluster by cluster.

6.1. RSGC1

Figer et al. (2006) reported on a cluster containing 14 RSGs, the RSGC1 located at $l = 25°3, b = -0°2$. High-resolution near-infrared spectroscopy confirmed their memberships (Davies et al. 2008). The 14 RSG stars have spectral types between K2 and M6. The mean radial velocity of the stars is 123.0 ± 1.0 km s^{-1}, while the velocity dispersion is 3.7 km s^{-1}, which yields a dynamical mass of a few times 10^4 $M_\odot$. With the derived kinematic distance of 6.6 ± 0.9 kpc, Davies et al. (2008) estimated luminosities $\log(L/L_\odot)$ from 4.87 to 5.45, which are consistent with a cluster age of 12 ± 2 Myr and initial masses of 18 $M_\odot$. We observed 8 of the 14 RSGs, for which we use the identification numbers introduced by Davies et al. (2008). We also included the nearby source X 18. This bright mid-infrared source was suggested to be a cluster member and possibly associated with the X-ray emitter AX J1838.0-0655 by Figer et al. (2006). Toward this source, located $2'$ south of the cluster, SiO emission was found by Nakashima & Deguchi (2006, (see below)). A radial velocity of 74 km s^{-1}, significantly lower than that of the stellar cluster, however, suggests non-membership (Nakashima & Deguchi 2006). Nakashima & Deguchi (2006) already searched for the SiO $v = 1$ and $v = 2, J = 1 - 0$ transitions at 43 GHz in the RSGs of RSGC1. They detected maser emission from

___

is always much weaker than the $v = 2, J = 1 - 0$ line and has not yet been reported in a RSG (Bujarrabal et al. 1996).
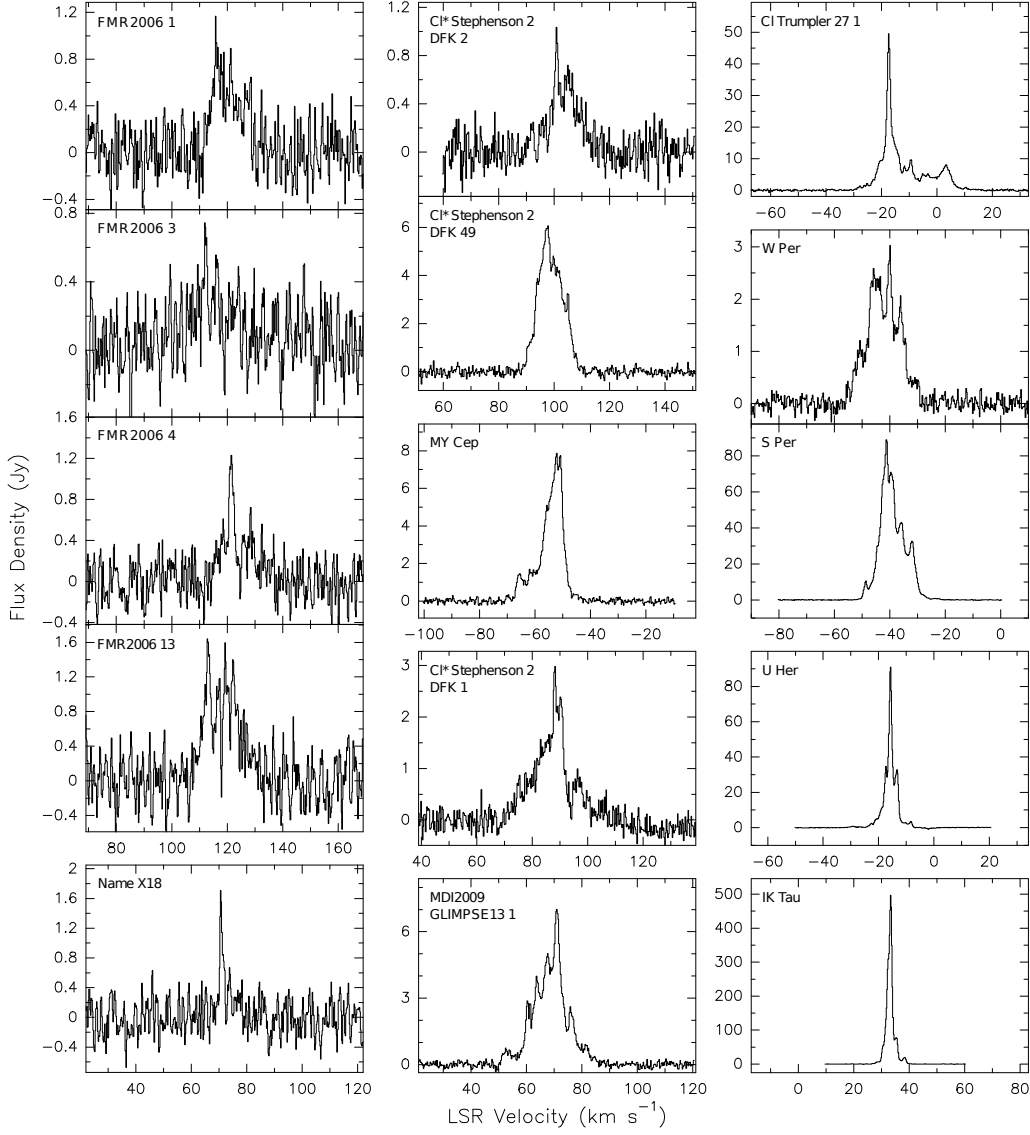
[3] http://simbad.u-strasbg.fr/simbad/

Fig. 1. Spectra of the SiO $v = 1$, $J = 2 - 1$ transition toward the stars were the line was detected. All stars but X 18, U Her, and IK Tau are RSGs. The latter two are Mira variables and we show their much narrower spectra for comparison.

four of the 14 RSGs: FMR2006 1, FMR2006 2, FMR2006 4 and FMR2006 13. Only the latter was detected in both transitions, the other three objects only showed the $v = 1$ line. Additionally, in a follow-up observation the 86 GHz $v = 1, J = 2 - 1$ SiO maser line was detected in FMR2006 1 and FMR2006 2. On top of that, Nakashima & Deguchi (2006) also found emission from both the $v = 1$ and $v = 2$ transitions toward X 18.

We detected 5 SiO masers in the direction of the RSGC1. We detected the $v = 1$, $J = 2 - 1$ transitions toward those objects found masing in the $J = 1 - 0$ lines by Nakashima & Deguchi (2006), except for FMR2006 2, which we did not observe (see Table 2). In addition, we made an additional detection, toward FMR2006 3. Our LSR velocities compare well with the values determined by Nakashima & Deguchi (2006).

We detected SiO maser emission toward X 18 with a velocity of 71 km s^{-1} (see Table 2), which makes its cluster membership highly unlikely. This value is in agreement with that measured at 43 GHz, i.e., 30 km s^{-1} below the

average cluster velocity. Were the maser star in a binary system, its velocity could deviate from the average cluster velocity. However, the agreement between the two radial velocities taken at two different epochs appears to discard this hypothesis. Nevertheless, it is tempting to speculate that X 18 is a higher energy version of the famous R Aqr symbiotic binary system. This system consists of an M-type AGB star and a compact object, most likely a white dwarf. It hosts a strong SiO maser (Zuckerman 1979) and shows radio and ultraviolet emission but, in contrast to X 18, is not very luminous in X rays (Viotti et al. 1987; Kafatos et al. 1989; Kellogg et al. 2007).

6.2. RSGC2

The RSGC2 was detected by Davies et al. (2007) as an overdensity of bright infrared stars in GLIMPSE and MSX images at $l = 26°2, b = 0°0$. Remarkably, a total of 26 cluster members are spectroscopically confirmed RSG stars (Davies et al. 2007) and have spectral types from K2 to

Table 4. Previous maser observations

Name	H₂O	SiO	OH	v_{LSR}	References	Comment
FMR2006 1		SiO		+115.0	(1)	
FMR2006 3						New
FMR2006 4		SiO		+121.5	(1)	
FMR2006 13		SiO		+116.5	(1)	
X 18		SiO		+74.3	(1)	
Stephenson 2 DFK 2	H₂O	SiO		+102.7	(2)	
Stephenson 2 DFK 49	H₂O	SiO		+98.6	(2)	
Stephenson 2 DFK 1	H₂O	SiO		+92.7	(2)	
NGC 7419-MY Cep	H₂O	SiO	OH	−55.8	(3),(4),(5)	
W Per	H₂O	SiO		-40.0	(6)	
S Per	H₂O	SiO	OH	-37.0	(4),(6)	
MDI2009 GLIMPSE13 1		SiO		+72.3	(2)	
Cl Trumpler 27 1		SiO			(7)	
IK Tau	H₂O	SiO	OH	+35.0	(4)	
U Her	H₂O	SiO	OH	−15.0	(4)	

References: (1) Nakashima & Deguchi (2006); (2) Deguchi et al. (2010); (3) Nakashima & Deguchi (2007); (4) Benson et al. (1990); (5) Takaba et al. (2001); (6) Valdettaro et al. (2001); (7) Hall et al. (1990).

Table 5. Comparison between RSG LSR velocities determined from SiO maser emission and IR CO absorption

Object	v_{LSR} [km s⁻¹]		
	previous (43 GHz SiO)	this study (86 GHz SiO)	CO (2.29 μm)
FMR2006 1	115[a]	116	130[g]
FMR2006 2	120[a]		114[g]
FMR2006 3		112	127[g]
FMR2006 4	121[a]	121	121[g]
FMR2006 13	116[a]	113	125[g]
X 18	74[a]	71	
Stephenson 2 DFK 2	103[b]	101	111[h]
Stephenson 2 DFK 49	101[b]	101	109[h]
Stephenson 2 DFK 1	93[b]	89	
MY Cep	-54[c]	-52	
W Per	-41[d]	-40	
S Per	-41[e]	-41	
MDI2009 GLIMPSE13 1	69/72[b]	71	
Cl Trumpler 27 1	-11[f]	-17	

Notes. Columns are (left to right): RSG designation and LSR velocities determined from the SiO $v = 1$, $J = 1 - 0$ and $2 - 1$ lines at 43 and 86 GHz, respectively, and the 2.29 μm CO bandhead absorption. References are:

References. [a] Nakashima & Deguchi (2006); [b] Deguchi et al. (2010); [c] Nakashima & Deguchi (2007); [d] Jiang et al. (1996); [d] Kim et al. (2010); [f] Haikala et al. (1994) – velocity based on 86 GHz SiO maser line; [g] Davies et al. (2008); [h] Davies et al. (2007).

M5. In order to host such a large number of RSGs implies a mass of 4×10^4 $M_\odot$ for this cluster. From the average radial velocity (109.3±0.7 km s⁻¹) a kinematic distance of $5.83^{+1.91}_{-0.78}$ kpc is inferred. By assuming this distance, and using theoretical models from Meynet & Maeder (2000), the authors derived a likely cluster age of 17±3 Myr (or 12± 1 when considering non-rotating isochrones). Luminosities $\log(L/L_\odot)$ of the RSGs range from 4.4 to 5.4, suggesting initial stellar masses of about 15 $M_\odot$ (Meynet & Maeder 2000). All 26 RSGs were included in our SiO maser search program. We used the identification numbers given by Davies et al. (2007). We also included star number one, which has been classified as a candidate RSG star in the

foreground of the cluster because of its brightness (K_S=2.9 mag) and radial velocity $\sim$ 95 km s⁻¹ (Davies et al. 2007).

Recently, Deguchi et al. (2010) performed an SiO $v = 1$ and $v = 2$, $J = 1-0$ maser search at 43 GHz in 18 objects of the RSGC2 cluster, resulting in five detections. Stephenson 2 DFK 1 and DFK 2 were detected only in the $v = 1$ transition, while DFK 22, DFK 49 and 2MASS J18385699-0606459 showed maser emission in both the $v = 1$ and $v = 2$ lines.

We detected three of the objects toward which Deguchi et al. (2010) found maser emission in the 43 GHz $J = 1 - 0$ lines: Stephenson 2 DFK 1, DFK 2 and DFK 49. The LSR velocities derived from the 43 GHz maser lines are within a few km s⁻¹ of the values we determine

for the $J = 2 - 1$ line, see Table 5. We note that star number 1, which has a significantly different velocity than the other two, is likely a field RSG, not associated with RSGC2 (Davies et al. 2007).

6.3. RSGC3

The RSGC3 was identified by Clark et al. (2009). It contains 8 RSGs with spectral types from K3 to M4, and 8 other candidate RSGs on the basis of photometric information. The number of RSGs suggests a cluster mass of about $2 \times 10^4 M_\odot$ - $4 \times 10^4 M_\odot$. The values of $\log(L/L_\odot)$ range from 4.5 and 4.8 when assuming a distance of 6 kpc, and suggest initial masses similar to those of the RSGs in RSGC2.

The target selection and IRAM observations presented here were carried out before completion of the analysis of Clark et al. (2009). The 8 spectroscopically confirmed RSGs and one of the candidate RSG were unsuccessfully searched for SiO masers. For those stars, we use the identification numbers given by Clark et al. (2009). Our list includes also 2MASS J18452254-0322261, which is not listed among the stellar members by Clark et al. (2009).

6.4. NGC 7419

Before the discovery of the RSGCs, the NGC 7419 cluster was the cluster with the largest number of known RSGs (Caron et al. 2003). The cluster is located at $l = 109°14, b = +1°14$ at a photometric distance of 2.3 ± 0.3 kpc (Beauchamp et al. 1994; Caron et al. 2003), and has an age of 25 ± 5 Myr (Subramaniam et al. 2006). Its four RSG members have spectral types from M2.5 to M7.5. We list these RSGs with the names provided in the SIMBAD database. The RSG MY Cep has already been detected in several maser surveys. It shows SiO, OH, and water masers (Nakashima & Deguchi 2007; Sivagnanam et al. 1990; Takaba et al. 2001).

We only found maser emission at 86 GHz toward the brightest member of the NGC7419 cluster, the M7.5 star MY Cep. SiO Maser emission at 43 GHz had been detected before by Nakashima & Deguchi (2007). They derived a radial velocity of -53.7 km s^{-1} from the $v = 1, J = 1 - 0$ transition and -51.9 km s^{-1} from the $v = 2, J = 1 - 0$ line. Our observations resulted in a very similar LSR velocity of -52 km s^{-1}. (see Table 5).

6.5. Perseus OB1

The Perseus OB1 association contains the famous double cluster h/χ Per. These young clusters (age ~14 My) have distances of $2.34^{+0.08}_{-0.08}$ kpc and $2.29^{+0.09}_{-0.08}$ kpc, respectively (Currie et al. 2010). The association contains at least 22 RSGs (Humphreys 1978; Garmany & Stencel 1992; Pierce et al. 2000). For one of them, S Per, recently a trigonometric parallax distance of $2.42^{+0.11}_{-0.09}$ kpc was measured (Asaki et al. 2010); see Xu et al. (2006) for another VLBI distance and a relevant discussion.

No SiO maser survey of the complete sample of RSGs in Per OB1 had been conducted so far. Only a few sources had been searched for SiO masers and maser emission was detected before in W Per (Jiang et al. 1996) and the well studied S Per, which is known for its strong maser emission

(e.g Kaifu et al. 1975). The ^{28}SiO $v = 1$ and $v = 2$, $J = 1-0$ and ^{29}SiO $v = 0$, $J = 1 - 0$ masers were searched for toward FZ Per and T Per, but no emission was detected (Jiang et al. 1999). SU Per was targeted in a SiO $v = 1$, $v = 2$ and $v = 3$, $J = 1-0$ search, but no maser was found (Spencer et al. 1981).

W Per was found to show emission in the 43 GHz $v = 1$, $J = 1-0$ transition (Jiang et al. 1996). S Per was observed by various authors in a number of transitions. The first detection was the $v = 1, J = 2 - 1$ line at 86 GHz by Kaifu et al. (1975). Furthermore, maser emission was found in the SiO $v = 1$, $v = 2$ and $v = 3$, $J = 1-0$ transitions (e.g. Spencer et al. 1977; Cho et al. 1996), the $v = 0$ and $v = 2$, $J = 2-1$ transitions (e.g Morris et al. 1979; Olofsson et al. 1981), and the $v = 1, J = 3 - 2$ transition (Herpin et al. 1998). Pardo et al. (1998) studied more than 15 different transitions of the SiO maser in S Per, detecting some high transitions such as $v = 2$ and $v = 3$, $J = 4 - 3$ and $v = 1$, $J = 5 - 4$.

The RSGs in the Perseus OB1 association discussed by Pierce et al. (2000) were part of our target list. We also observed the brightest member of the NGC 457 cluster, which is a M1.5 Iab star (Mermilliod et al. 2008).

We detected SiO maser emission toward two RSGs in the Per OB1 association, W Per and S Per. Both sources were known to host masers (see above). The detected stars are among the three RSG members with longer periods and have redder colors of 485 and 822 days, respectively. This led Pierce et al. (2000) to suggest that these objects are surrounded by a CSE.

We obtain an LSR velocity of -41 km s^{-1} for S Per and -40 km s^{-1} for W Per, respectively (see Table 2). Jiang et al. (1996) reported -41.3 km s^{-1} for W Per based on their 43 GHz maser observations, in agreement with our findings. For S Per, several results can be found in the literature that agree within a km s^{-1} with our value (Alcolea et al. 1990; Kim et al. 2010).

6.6. GLIMPSE13

The GLIMPSE13 cluster contains a large number of spectroscopically confirmed G9 and M1 stars (Messineo et al. 2009; Mercer et al. 2005). including suspected supergiants with spectral types ranging from early K to late G. Since yellow supergiants are rarer than RSGs, and Galactic RSGs have a median spectral type of M2, it is more likely that the stars in GLIMPSE13 are massive giants with an age between 50 and 100 Myr (Messineo et al. 2009). The bright star GLIMPSE13 1, however, is too luminous to be a giant member of the same cluster (K_S=2.67 mag) and is of type M0I or M7III.

GLIMPSE13 was targeted in the searches for SiO and water masers in stellar clusters conducted by Deguchi et al. (2010). There is only an overlap of two sources with the stars for which Messineo et al. (2009) report IR data. Deguchi et al. (2010) detected three SiO masing stars (including GLIMPSE13 1, our one target star) with radial velocities around 70 km s^{-1} (72.3, 74.9 and 70.2 km s^{-1}), and they found water maser emission with a velocity of 21.4 km s^{-1} toward GLIMPSE13 2 (a K5III star). A velocity of 71 km s^{-1} corresponds to a near-kinematic distance of $4.3^{+0.37}_{-0.36}$ kpc, while a velocity of 21 km s^{-1} implies a distance of 1.6 ± 0.4 kpc. The cluster is located in a particularly rich portion of the disk at a longitude of 33.8°. Several

young stellar objects are located a few arcminutes north of the cluster, and a number of bright mid-infrared sources surround the cluster. It is most likely that we are seeing different groups of stars along neighboring lines-of-sight that are not physically associated.

We detected SiO maser emission in the $v = 1, J = 2 - 1$ line in the RSG candidate GLIMPSE13 1. Maser emission at 43 GHz had been observed before by Deguchi et al. (2010) in the $v = 1, J = 1 - 0$ transition. They found LSR velocities of peak emission of 69.4 km s^{-1} and 72.3 km s^{-1} on two separate observing days, completely in agreement with our value of 71 km s^{-1} (see Table 2). The SiO maser lines' shape and breadth suggest that GLIMPSE13 1 is a RSG. The mean equivalent width of the maser emission is 27 km s^{-1}.

6.7. GLIMPSE9

The stellar cluster number 9 in the list of Mercer et al. (2005) was analyzed with near-infrared spectroscopy and HST/NICMOS photometry by Messineo et al. (2009). These authors detected 3 RSG stars and one late M giant (or early type RSG). The cluster is located at a spectro-photometric distance of 4.2 kpc, has a likely age of 15-27 Myr, and a cluster mass of at least 1600 $M_{\odot}$.

We included in our target list all 4 late-type stars detected in the direction of the GLIMPSE9 cluster (3 RSGs and 1 giant). Maser lines were not detected.

6.8. SGR 1900+14

We also included among the targets the two RSG stars that are members of the stellar cluster associated with the magnetar (soft gamma ray repeater) SGR1900+14 (Davies et al. 2009a). The cluster is located at a kinematic distance of 12.5 ± 1.7 kpc, and has a likely age of 14 Myr. The two M5I stars have an angular separation of just $\sim 2''$. Therefore only a single pointing was needed with the IRAM 30m telescope. Maser lines were not detected.

6.9. MFD2008 (Cl 1813-178)

A young massive cluster was recently identified in the direction of the W33 complex at a kinematic distance of about 4 kpc. It contains several evolved early-type stars and 1 RSG (Messineo et al. 2008, 2011), from which a likely age of 4.5 Myr and a cluster mass of 10^4 $M_{\odot}$ are inferred. We included among our targets the RSG identified in the MFD2008 cluster by Messineo et al. (2008). We did not detect SiO maser emission toward this cluster member.

6.10. Trumpler 27

The Trumpler 27 cluster is located at $l = 335°.1, b = -0°.7$ at a spectro-photometric distance of 2.1 ± 0.2 kpc (Moffat et al. 1977). It contains a binary RSG of M0 type (Massey et al. 2001). The presence of two Wolf Rayet stars and several other evolved OB stars suggests a cluster age below 6 Myr. We included in our program the RSG. The 43 GHz $v = 1, J = 1 - 0$ transition was already observed by Hall et al. (1990). The 86 GHz $v = 1, J = 2 - 1$ line was also found before (Haikala et al. 1994).

We detected SiO maser emission at 86 GHz toward the binary RSG in Trumpler 27. We determine an LSR velocity of -17 km s^{-1} (see Table 2), slightly higher than the -11 km s^{-1} reported by Haikala et al. (1994).

6.11. The Galactic center and Inner Galaxy RSGs not associated with clusters

Blum et al. (2003) performed a spectro-photometric analysis of a sample of 79 luminous late-type stars in the central parsecs of the Galaxy. We observed 7 out of the 17 RSGs listed by Blum et al. (2003), but no maser lines were detected. One of the sources, BSD96 66, is the famous IRS 7, the brightest near IR source in the central parsec (Becklin & Neugebauer 1975). Toward this source, Menten et al. (1997) detected the 43.3 GHz $v = 1, J = 1 - 0$ SiO line with the NRAO Very Large Array (VLA) with a peak flux density of 0.38 Jy. Given that the 43 and 86 GHz $v = 1$ maser fluxes are comparable (see Sect. 7.3), it is not surprising that we did not obtain a detection given our noise level (0.22 Jy; see Table 3).

With a similar technique, Comerón et al. (2004) identified 18 RSGs located in the Inner Galaxy. We observed nine of these RSGs, but maser emission was not detected.

6.12. Clusters without SiO maser detections – summary

With our average rms noise of 0.23 Jy, we report the first unsuccessful searches toward targets in RSGC3, GLIMPSE9, MFD2008 and SGR 1900+14, as well as the isolated RSGs (Blum et al. 2003; Comerón et al. 2004) discussed in Sect. 6.11 (see Table 3). SiO masers vary with pulsation phase (e.g. Alcolea et al. 1990, 1999). New and deeper SiO maser observations could be useful to detect possible maser emission.

7. Analysis

7.1. Line equivalent widths

For comparison, we also observed the maser emission from the Mira variables IK Tau and U Her. From Table 2 and Fig. 1, it is obvious that the emission from the Miras, while very strong because close to Earth (~ 100 pc), covers much smaller velocity intervals than the RSGs' emission. The SiO maser lines in RSGs are generally broader than those in Mira stars (e.g. Le Bertre & Nyman 1990; within errors our new data confirms this previous result). Fig. 2 shows a histogram of the velocity range covered by the SiO maser line. The Mira variables IK Tau and U Her are shown in a grey color. Clearly, their profiles are much narrower than those of the bulk of the RSG's. Alcolea et al. (1990) found the mean equivalent width, given by (profile-area)/(peak-intensity), of the 86 GHz SiO maser lines to be 8.6 km s^{-1} (rms of 1.3 km s^{-1}) for their sample of 10 RSGs, and only 4 km s^{-1} (rms of 1 km s^{-1}) for the 17 Miras. In our case, using the values of Table 2, the 13 RSGs have a mean equivalent width of 7.4 km s^{-1} (rms of 2.7 km s^{-1}), while the 2 Miras have a width of 2.4 km s^{-1} (rms of 0.4 km s^{-1}).

Since for a CSE created by mass outflow, the terminal expansion velocity is proportional to the mass loss rate, the higher line widths we find for the RSGs (compared to Miras), simply reflects their greater degree of mass loss.
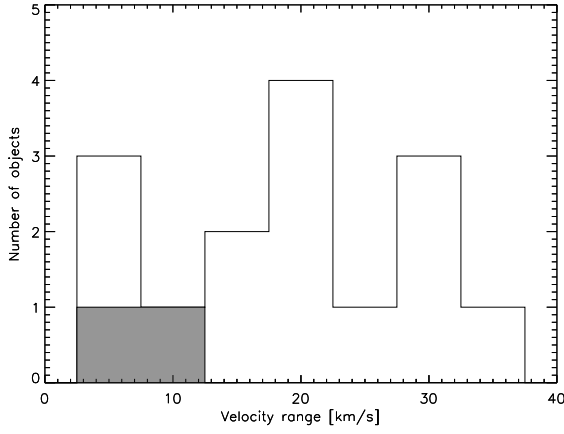
Fig. 2. Histogram of the LSR velocity range covered by the maser emission. The grey region shows the Mira variables IK Tau and U Her.

Fig. 3. The two extinction-free parameters Q1 and Q2 are plotted. Small dots indicate SiO maser detections by Messineo et al. (2002). Empty hexagons are our targeted RSGs without maser detections, and filled hexagons are those with maser emission.

7.2. Maser occurrence versus the Q1 and Q2 parameters

With a combination of near- and mid-IR colors it is possible to identify mass-losing stars and to distinguish between highly reddened "naked" stars and dust-enshrouded stars. Messineo et al. (2012) proposed a new source selection method for identifying mass-losing late-type stars, which is based on photometric data from 2MASS and GLIMPSE (Cutri et al. 2003; Benjamin et al. 2003) and on the $Q1$ and $Q2$ parameters. These two parameters are independent of interstellar extinction. The $Q1$ parameter ($Q1 = (J - H) - 1.8 \times (H - K_S)$) is a measure of the deviation from the reddening vector in the 2MASS ($J - H$) versus ($H - K_S$) plane ($H, J,$ and K_S are the stars' magnitudes in the corresponding IR bands). Early-type stars have $Q1$ values around 1 and K-giants around 0.4 mag. Dusty circumstellar envelopes change the energy distribution of late-type stars, and generate smaller $Q1$ values. On average, higher mass-loss rates produce smaller $Q1$ values (see trend in Fig. 4 by Messineo et al. 2012). Similarly, the $Q2$ parameter ($Q2 = (J - K_S) - 2.69 \times (K_S - [8.0])$) measures the deviation from the interstellar vector in the 2MASS/GLIMPSE plane ($J - K_S$) versus ($K_S - [8.0]$). On average, higher mass-loss rates imply smaller $Q2$ values (see trends in Figs. 2 and 6 by Messineo et al. 2012).

A plot of the $Q1$ versus $Q2$ parameters for the targeted RSGs is shown in Fig. 3. It shows that with our sensitivity we were able to detect masers only in stars with $Q2$ values smaller than -1.9 mag. This implies that SiO maser emission was detected toward the reddest sources, and supports a radiative pumping mechanism for the SiO masers in RSGs (Alcolea et al. 1990). For comparison, points representing the SiO maser star sample of Messineo et al. (2002) are also plotted in Fig. 3. The corresponding data were taken with the same telescope as for our sample and have similar rms noise. However, the Messineo et al. sample is composed of Mira-like AGB stars, i.e. of stars of luminosity class III, (Messineo et al. 2004, 2005), while our new data points represent RSGs (luminosity class I).

There is an interesting shift between the $Q2$ values of masing sources from the one to the other sample. This suggests that higher mass-loss rates are required for RSGs to show SiO maser action than for AGB stars. Perhaps, the
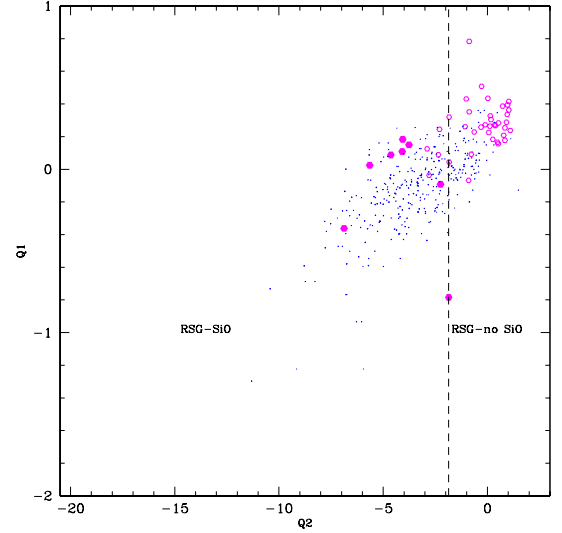
higher luminosities of RSGs push the dust condensation radius and the masing shell farther out. Mass-loss is indeed proportional to density and envelope size (see equation A3 in Sevenster 1999). A large statistics is needed to confirm this suggested color threshold.

7.3. SiO maser intensities

In Table 6, we list the ratio of the 43 GHz peak flux from the literature over the 86 GHz peak flux derived here. Apart from IK Tau, MY Cep and Cl* Stephenson 2 DFK 2, the 86 GHz transition is found to be stronger in all sources. The mean value of the 43/86 GHz ratio is 0.73 with a standard deviation of 0.41. This makes the 86 GHz transition a good line for determining radial velocities of RSG stars. Nyman et al. (1993) concluded that the 43 GHz over 86 GHz ratio increases with increasing mass-loss rates. Values above average are measured for MY Cep and DFK 2. We should note, however, that the SiO maser intensity is found to vary during the stellar variability cycle (e.g. Alcolea et al. 1990, 1999). The 43 GHz and 86 GHz observations are not simultaneously taken, and their peak intensities could vary with stellar phase. Therefore, the individual ratios may be not conclusive, and a simultaneous detection program should be carried out. A large fraction of stars have ratios below unity, confirming that with single dish telescopes surveys for 86 GHz SiO maser emission are more efficient than for 43 GHz emission. One should however, note that the VLA has been a very sensitive instrument for 43 GHz SiO maser searches (see Menten et al. 1997) and its expanded version, the Karl G. Jansky Very Large Array (JLVA) will be even more so. However, its sensitivity will be matched by the Atacama Large Millimeter Array (ALMA), which (after completion) will cover both lines with formidable sensitivity for sources with declinations up to $\sim 40°$.

Table 6. Maser/maser and maser/8 μm IR continuum flux ratios

Object	F_{43GHz}/F_{86GHz}	$F_{86GHz}/F_{8\mu m}$	Ref. 43 GHz
FMR2006 1	0.76	. . .	(1)
FMR2006 3	. . .	. . .	
FMR2006 4	0.89	. . .	(1)
FMR2006 13	0.89	0.18	(1)
X 18	0.95	0.90	(1)
Stephenson 2 DFK 2	1.26	0.08	(2)
Stephenson 2 DFK 49	0.95	0.82	(2)
Stephenson 2 DFK 1	0.35	0.10	(2)
NGC 7419/MY Cep	1.38	0.09	(3)
W Per	0.41	. . .	(4)
S Per	0.21	. . .	(5)
MDI2009 GLIMPSE13 1	0.41	0.07	(2)
Cl Trumpler 27 1	0.16	0.33	(6)
IK Tau (Mira)	1.22	. . .	(7)
U Her (Mira)	0.37	. . .	(7)

Notes. Columns are (from left to right) designations of the targeted RSGs ratios of SiO(43 GHz peak flux)/SiO(86 GHz peak flux) ratio and SiO(86 GHz peak flux)/IR(8 μm flux) (see Alcolea et al. 1990). The 8 μm fluxes are taken from the MSX and GLIMPSE catalogue. Sources without measurements were not included in these surveys, or saturated in GLIMPSE. References are:

References. (1) Nakashima & Deguchi (2006); (2) Deguchi et al. (2010); (3) Nakashima & Deguchi (2007); (4) Jiang et al. (1996); (5) Cho et al. (1996); (6) Hall et al. (1990); (7) Kim et al. (2010).

We also calculated the ratio of the 86 GHz peak flux over the IR 8 μm peak flux (see Table 6). The 8 μm fluxes were taken from the MSX (Price et al. 2001) and GLIMPSE (Benjamin et al. 2003) catalogues when available. Previously, Alcolea et al. (1990) performed a SiO maser search in Miras and supergiants, and found a SiO(86 GHz peak flux)/IR(8μm flux) ratio $\sim 1/5$ for Miras and the RSGs with the strongest maser emission, but significantly lower for the other supergiants (with 0.003 for SW Vir being the lowest ratio). We find a mean value of 0.32 for the 86 GHz peak flux over the 8 μm flux ratio (standard deviation of 0.34). Clearly, for all stars, the SiO maser flux is smaller than the 8 μm flux. Therefore they meet the criterion required by a radiative pump, which was established by the modeling of SiO maser pumping schemes; see Sect. 3.1. Again, we should note that both SiO maser and IR flux, which both are variable, generally were not measured contemporaneously.

8. Conclusions

We performed an extensive search for the SiO $v = 1$, $J = 2 - 1$ maser line at 86 GHz in 88 (candidate) RSGs in Galactic open clusters. Most of these stellar clusters were never before covered covered by a 86 GHz SiO maser survey. In total, we detected maser emission from 13 RSGs, 1 of which is the first detection on any SiO in the respective object. The measurements provide accurate LSR velocities, which can be used in studies of the Galactic structure. For the clusters containing masing stars, our non-detection of SiO emission in other RSG members may, in combination with a well determined distance to the cluster, yield information on the fraction of RSGs with high enough mass-loss to form maser containing CSEs or a dependence on maser occurrence with spectral type.

The FWHMs of the SiO maser lines are broader in RSGs than in Mira AGBs. The intensities of the 86 GHz SiO maser lines are somewhat stronger than those of 43 GHz $v = 1$, $J = 1-0$ SiO maser lines in most the sources (11 out of the 14 known to be masing in both lines). The JVLA and ALMA will provide all sky coverage for extremely sensitive surveys in both lines.

SiO maser emission was detected in targets with $Q2$ values larger than ~ -2 mag. This increase of the detection rate with redder colors supports a radiative pumping mechanism for the SiO maser. The $Q1$ and $Q2$ parameters are proven to be useful tools for efficient targeted searches for SiO masers.

References

Alcolea, J., Bujarrabal, V., & Gomez-Gonzalez, J. 1990, A&A, 231, 431
Alcolea, J., Pardo, J. R., Bujarrabal, V., et al. 1999, A&AS, 139, 461
Alexander, M. J., Kobulnicky, H. A., Clemens, D. P., et al. 2009, AJ, 137, 4824
Asaki, Y., Deguchi, S., Imai, H., et al. 2010, ApJ, 721, 267
Beauchamp, A., Moffat, A. F. J., & Drissen, L. 1994, ApJS, 93, 187
Becklin, E. E. & Neugebauer, G. 1975, ApJ, 200, L71
Benjamin, R. A., Churchwell, E., Babler, B. L., et al. 2003, PASP, 115, 953
Benson, P. J., Little-Marenin, I. R., Woods, T. C., et al. 1990, ApJS, 74, 911
Bissantz, N., Englmaier, P., & Gerhard, O. 2003, MNRAS, 340, 949
Blum, R. D., Ramírez, S. V., Sellgren, K., & Olsen, K. 2003, ApJ, 597, 323
Buhl, D., Snyder, L. E., Lovas, F. J., & Johnson, D. R. 1974, ApJ, 192, L97

Bujarrabal, V. 1994a, A&A, 285, 953

Bujarrabal, V. 1994b, A&A, 285, 971

Bujarrabal, V., Alcolea, J., Sanchez Contreras, C., & Colomer, F. 1996, A&A, 314, 883

Bujarrabal, V., Planesas, P., & del Romero, A. 1987, A&A, 175, 164

Caron, G., Moffat, A. F. J., St-Louis, N., Wade, G. A., & Lester, J. B. 2003, AJ, 126, 1415

Cho, S.-H., Kaifu, N., & Ukita, N. 1996, A&AS, 115, 117

Choi, Y. K., Hirota, T., Honma, M., et al. 2008, PASJ, 60, 1007

Clark, J. S., Negueruela, I., Crowther, P. A., & Goodwin, S. P. 2005, A&A, 434, 949

Clark, J. S., Negueruela, I., Davies, B., et al. 2009, A&A, 498, 109

Comerón, F., Torra, J., Chiappini, C., et al. 2004, A&A, 425, 489

Cotera, A. S., Erickson, E. F., Colgan, S. W. J., et al. 1996, ApJ, 461, 750

Currie, T., Hernandez, J., Irwin, J., et al. 2010, ApJS, 186, 191

Cutri, R. M., Skrutskie, M. F., van Dyk, S., et al. 2003, 2MASS All Sky Catalog of point sources. (NASA)

Davies, B., Figer, D. F., Kudritzki, R., et al. 2007, ApJ, 671, 781

Davies, B., Figer, D. F., Kudritzki, R., et al. 2009a, ApJ, 707, 844

Davies, B., Figer, D. F., Law, C. J., et al. 2008, ApJ, 676, 1016

Davies, B., Origlia, L., Kudritzki, R., et al. 2009b, ApJ, 696, 2014

Deguchi, S., Fujii, T., Nakashima, J.-I., & Wood, P. R. 2002, PASJ, 54, 719

Deguchi, S., Nakashima, J., Zhang, Y., et al. 2010, PASJ, 62, 391

Elitzur, M. 1980, ApJ, 240, 553

Epchtein, N., Deul, E., Derriere, S., et al. 1999, VizieR Online Data Catalog, 1, 2002

Figer, D. F., Kim, S. S., Morris, M., et al. 1999, ApJ, 525, 750

Figer, D. F., MacKenty, J. W., Robberto, M., et al. 2006, ApJ, 643, 1166

Figer, D. F., Najarro, F., Gilmore, D., et al. 2002, ApJ, 581, 258

Figer, D. F., Rich, R. M., Kim, S. S., Morris, M., & Serabyn, E. 2004, ApJ, 601, 319

Garmany, C. D. & Stencel, R. E. 1992, A&AS, 94, 211

Habing, H. J. 1996, A&A Rev., 7, 97

Habing, H. J., Sevenster, M. N., Messineo, M., van de Ven, G., & Kuijken, K. 2006, A&A, 458, 151

Haikala, L. K., Nyman, L., & Forsstroem, V. 1994, A&AS, 103, 107

Hall, P. J., Allen, D. A., Troup, E. R., Wark, R. M., & Wright, A. E. 1990, MNRAS, 243, 480

Harwit, M., Malfait, K., Decin, L., et al. 2001, ApJ, 557, 844

Herpin, F., Baudry, A., Alcolea, J., & Cernicharo, J. 1998, A&A, 334, 1037

Heske, A. 1989, A&A, 208, 77

Humphreys, E. M. L. 2007, in IAU Symposium, Vol. 242, IAU Symposium, ed. J. M. Chapman & W. A. Baan, 471–480

Humphreys, E. M. L., Gray, M. D., Yates, J. A., et al. 2002, A&A, 386, 256

Humphreys, R. M. 1978, ApJS, 38, 309

Jewell, P. R., Snyder, L. E., Walmsley, C. M., Wilson, T. L., & Gensheimer, P. D. 1991, A&A, 242, 211

Jiang, B. W., Deguchi, S., & Ramesh, B. 1999, PASJ, 51, 95

Jiang, B. W., Deguchi, S., Yamamura, I., et al. 1996, ApJS, 106, 463

Kafatos, M., Hollis, J. M., Yusef-Zadeh, F., Michalitsianos, A. G., & Elitzur, M. 1989, ApJ, 346, 991

Kaifu, N., Buhl, D., & Snyder, L. E. 1975, ApJ, 195, 359

Kellogg, E., Anderson, C., Korreck, K., et al. 2007, ApJ, 664, 1079

Kim, J., Cho, S.-H., Oh, C. S., & Byun, D.-Y. 2010, ApJS, 188, 209

Kwan, J. & Scoville, N. 1974, ApJ, 194, L97

Le Bertre, T. & Nyman, L. 1990, A&A, 233, 477

Levesque, E. M. 2010, in Astronomical Society of the Pacific Conference Series, Vol. 425, Hot and Cool: Bridging Gaps in Massive Star Evolution, ed. C. Leitherer, P. D. Bennett, P. W. Morris, & J. T. Van Loon, 103

Lockett, P. & Elitzur, M. 1992, ApJ, 399, 704

Massey, P., DeGioia-Eastwood, K., & Waterhouse, E. 2001, AJ, 121, 1050

Menten, K. M., Lundgren, A., Belloche, A., Thorwirth, S., & Reid, M. J. 2008, A&A, 477, 185

Menten, K. M., Reid, M. J., Eckart, A., & Genzel, R. 1997, ApJ, 475, L111

Mercer, E. P., Clemens, D. P., Meade, M. R., et al. 2005, ApJ, 635, 560

Mermilliod, J. C., Mayor, M., & Udry, S. 2008, A&A, 485, 303

Messineo, M., Davies, B., Figer, D. F., et al. 2011, ApJ, 733, 41

Messineo, M., Davies, B., Ivanov, V. D., et al. 2009, ApJ, 697, 701

Messineo, M., Figer, D. F., Davies, B., et al. 2008, ApJ, 683, L155

Messineo, M., Habing, H. J., Menten, K. M., Omont, A., & Sjouwerman, L. O. 2004, A&A, 418, 103

Messineo, M., Habing, H. J., Menten, K. M., et al. 2005, A&A, 435, 575

Messineo, M., Habing, H. J., Sjouwerman, L. O., Omont, A., & Menten, K. M. 2002, A&A, 393, 115

Messineo, M., Menten, K. M., Churchwell, E., & Habing, H. 2012, A&A, 537, A10

Meynet, G. & Maeder, A. 2000, A&A, 361, 101

Moffat, A. F. J., Fitzgerald, M. P., & Jackson, P. D. 1977, ApJ, 215, 106

Morris, M., Redman, R., Reid, M. J., & Dickinson, D. F. 1979, ApJ, 229, 257

Nakashima, J. & Deguchi, S. 2006, ApJ, 647, L139

Nakashima, J. & Deguchi, S. 2007, ApJ, 669, 446

Negueruela, I., González-Fernández, C., Marco, A., & Clark, J. S. 2011, A&A, 528, A59+

Negueruela, I., González-Fernández, C., Marco, A., Clark, J. S., & Martínez-Núñez, S. 2010, A&A, 513, A74+

Nguyen Luong, Q., Motte, F., Schuller, F., et al. 2011, A&A, 529, A41

Nyman, L.-A., Hall, P. J., & Le Bertre, T. 1993, A&A, 280, 551

Olofsson, H., Rydbeck, O. E. H., Lane, A. P., & Predmore, C. R. 1981, ApJ, 247, L81

Pardo, J. R., Cernicharo, J., Gonzalez-Alfonso, E., & Bujarrabal, V. 1998, A&A, 329, 219

Pierce, M. J., Jurcevic, J. S., & Crabtree, D. 2000, MNRAS, 313, 271

Price, S. D., Egan, M. P., Carey, S. J., Mizuno, D. R., & Kuchar, T. A. 2001, AJ, 121, 2819

Reid, M. J., Menten, K. M., Zheng, X. W., et al. 2009, ApJ, 700, 137

Scholz, M. & Wood, P. R. 2000, A&A, 362, 1065

Sevenster, M. N. 1999, MNRAS, 310, 629

Sivagnanam, P., Le Squeren, A. M., Minh, F. T., & Braz, M. A. 1990, A&A, 233, 112

Spencer, J. H., Schwartz, P. R., Waak, J. A., & Bologna, J. M. 1977, AJ, 82, 706

Spencer, J. H., Schwartz, P. R., Winnberg, A., et al. 1981, AJ, 86, 392

Stephenson, C. B. 1990, AJ, 99, 1867

Subramaniam, A., Mathew, B., Bhatt, B. C., & Ramya, S. 2006, MNRAS, 370, 743

Takaba, H., Iwate, T., Miyaji, T., & Deguchi, S. 2001, PASJ, 53, 517

Valdettaro, R., Palla, F., Brand, J., et al. 2001, A&A, 368, 845

Verhoelst, T., van der Zypen, N., Hony, S., et al. 2009, A&A, 498, 127

Viotti, R., Piro, L., Friedjung, M., & Cassatella, A. 1987, ApJ, 319, L7

Westerlund, B. 1961, PASP, 73, 51

Xu, Y., Reid, M. J., Zheng, X. W., & Menten, K. M. 2006, Science, 311, 54

Zuckerman, B. 1979, ApJ, 230, 442

Table 3. Red Supergiants without SiO $v = 1; J = 2 - 1$ detection.

Object	α_{J2000} [J2000]	δ_{J2000} [J2000]	rms [Jy]
Figer et al. (2006, RSGC1 cluster)			
FMR2006 11	18:37:51.72	-06:51:49.9	0.497
FMR2006 12	18:38:03.30	-06:52:45.1	0.499
FMR2006 14	18:37:47.64	-06:53:02.3	0.567
FMR2006 16	18:38:01.29	-06:52:51.9	0.590
Davies et al. (2007, RSGC2 cluster)			
Stephenson 2 DFK 3	18:39:24.60	-06:02:13.8	0.186
Stephenson 2 DFK 5	18:39:08.10	-06:05:24.4	0.192
Stephenson 2 DFK 6	18:39:18.40	-06:00:38.4	0.320
Stephenson 2 DFK 8	18:39:19.90	-06:01:48.1	0.325
Stephenson 2 DFK 9	18:39:06.80	-06:03:20.3	0.332
Stephenson 2 DFK 10	18:39:14.70	-06:01:36.6	0.338
Stephenson 2 DFK 11	18:39:18.30	-06:02:14.3	0.331
Stephenson 2 DFK 13	18:39:17.70	-06:04:02.5	0.337
Stephenson 2 DFK 14	18:39:20.40	-06:01:42.6	0.339
Stephenson 2 DFK 15	18:39:22.40	-06:01:50.1	0.351
Stephenson 2 DFK 16	18:39:24.00	-06:03:07.3	0.352
Stephenson 2 DFK 17	18:39:15.10	-06:05:19.1	0.342
Stephenson 2 DFK 18	18:39:22.50	-06:00:08.4	0.363
Stephenson 2 DFK 19	18:39:19.50	-05:59:19.4	0.371
Stephenson 2 DFK 20	18:39:24.10	-06:00:22.8	0.378
Stephenson 2 DFK 21	18:39:15.80	-06:02:05.5	0.369
Stephenson 2 DFK 23	18:39:01.50	-06:00:59.9	0.396
Stephenson 2 DFK 26	18:39:35.10	-05:59:15.8	0.410
Stephenson 2 DFK 27	18:39:16.00	-06:05:03.2	0.431
Stephenson 2 DFK 29	18:39:22.20	-06:02:14.7	0.460
Stephenson 2 DFK 30	18:39:23.40	-05:59:01.3	0.489
Stephenson 2 DFK 31	18:39:09.30	-06:01:06.9	0.527
Stephenson 2 DFK 52	18:39:23.40	-06:02:15.9	0.571
Stephenson 2 DFK 72	18:39:16.20	-06:03:07.2	0.624
Clark et al. (2009, RSG3 cluster)			
CND2009 S1	18:45:23.60	-03:24:13.9	0.316
CND2009 S2	18:45:26.54	-03:23:35.4	0.196
CND2009 S3	18:45:24.35	-03:22:42.1	0.176
CND2009 S4	18:45:25.32	-03:23:01.1	0.155
CND2009 S5	18:45:23.27	-03:23:44.1	0.313
CND2009 S7	18:45:24.18	-03:23:47.4	0.238
CND2009 S8	18:45:20.06	-03:22:47.2	0.309
CND2009 S9	18:45:28.13	-03:22:54.6	0.303
CND2009 S14	18:45:29.03	-03:22:37.4	0.306
2MASS J18452254-0322261	18:45:22.54	-03:22:26.1	0.307
Caron et al. (2003, NGC 7419)			
NGC 7419 BMD 435	22:54:16.14	+60:49:29.0	0.138
NGC 7419 BMD 696	22:54:22.67	+60:48:31.7	0.146
NGC 7419 BMD 921	22:54:30.49	+60:47:50.7	0.149
NGC 7419 BMD 139	22:54:01.28	+60:47:42.0	0.154
Pierce et al. (2000); Mermilliod et al. (2008, Per OB1)			
FZ Per (NGC 884 MMU 1818)	02:20:20.60	+57:09:31.0	0.158
RS Per (NGC 884 2417)	02:22:24.30	+57:06:34.0	0.153
AD Per (NGC 884 MMU 1655)	02:20:29.00	+56:59:35.0	0.151
GP Cas	02:39:50.40	+59:35:51.0	0.156
T Per	02:19:21.90	+58:57:40.0	0.152
YZ Per	02:38:25.40	+57:02:46.0	0.150
BU Per (NGC 869 MMU 899)	02:18:53.30	+57:25:17.0	0.140
V500Cas	02:51:24.00	+57:50:00.0	0.138
XX Per	02:03:09.40	+55:13:57.0	0.143
SU Per	02:22:06.90	+56:36:14.0	0.111
V466 Cas (NGC 457 25)	01:19:53.64	+58:18:31.2	0.138
Messineo et al. (2009, GLIMPSE9)			
MFD2010 1	18:34:09.27	-09:14:00.7	0.159
MFD2010 5	18:34:09.87	-09:14:23.3	0.166
MFD2010 6	18:34:10.37	-09:13:49.5	0.180
MFD2010 8	18:34:10.36	-09:13:52.9	0.160
Davies et al. (2009a, SGR 1900+14)			
VLH96 A & VLH96 B	19:07:15.35	+09:19:21.4	0.165
Messineo et al. (2008, MFD2008)			

MFD2008 1	18:13:22.26	-17:54:15.6	0.165
Blum et al. (2003, Galactic center)			
BSD96 1	17:45:36.93	-29:00:30.2	0.210
BSD96 14	17:45:38.52	-28:59:56.8	0.206
BSD96 48	17:45:39.69	-29:00:54.2	0.210
BSD96 66	17:45:39.99	-29:00:22.2	0.217
BSD96 79	17:45:40.14	-28:59:39.5	0.198
BSD96 108	17:45:41.08	-29:00:47.9	0.205
BSD96 109	17:45:41.12	-29:00:39.6	0.216
Comerón et al. (2004, RSGs in the inner Galaxy)			
CTC2004 64	18:07:50.72	-20:04:09.2	0.155
CTC2004 70	18:08:37.35	-19:50:05.3	0.152
CTC2004 74	18:09:37.50	-19:28:27.1	0.151
CTC2004 97	18:14:53.10	-17:00:51.3	0.147
CTC2004 121	18:16:38.18	-16:23:34.0	0.151
CTC2004 125	18:16:55.97	-16:09:54.3	0.157
CTC2004 152	18:18:05.31	-15:57:19.4	0.160
CTC2004 184	18:25:11.20	-12:28:40.2	0.154
CTC2004 194	18:27:39.07	-11:39:23.0	0.161

Columns are (from left to right) designations of the targeted RSGs (names are taken from SIMBAD), right ascension, declination, and rms noise.